Research Square

Preprints are preliminary reports that have not undergone peer review.
They should not be considered conclusive, used to inform clinical practice,
or referenced by the media as validated information.

Genomic Characterization and Functional Validation of Microencapsulated Fibrinolytic Proteases Produced By Bacillus pacificus HSFI-5

Stalis Norma Ethica

norma@unimus.ac.id

Magister of Public Health, Universitas Muhammadiyah Semarang

Yumitha Sakinah Putri

Universitas Bhakti Pertiwi Indonesia

Wessal Houali

Texas Tech University

Dewi Seswita Zilda

National Research and Innovation Agency

Marlyn Dian Laksitorini

Universitas Gadjah Mada

Sri Rejeki

Universitas Muhammadiyah Semarang

Samuel Tanoeyadi

Oregon State University

Taifo Mahmud

Oregon State University

Research Article

Keywords: Bacillus pacificus, coagulation, D-dimer, enzyme microencapsulation, fibrinolytic protease, microbial enzyme biotechnology, whole genome sequencing

Posted Date: March 3rd, 2026

DOI: https://doi.org/10.21203/rs.3.rs-8930375/v1

License: This work is licensed under a Creative Commons Attribution 4.0 International License.
Read Full License

Additional Declarations: No competing interests reported.

Abstract

Microbial fibrinolytic proteases offer significant potential for breaking down degradation in biotechnology applications. In this study, we used whole-genome sequencing and bioactivity assays to examine microencapsulated extracellular fibrinolytic proteases from *Bacillus pacificus* HSFI-5. Sequencing on the Illumina and MGI platforms identified at least 7 protease genes, including *vpr*, *aprE*, and *inha*, linked to fibrinolytic activity. Both platforms produced similar genome sizes (about 5.45–5.48 Mb) and GC contents (about 35.3%), showing consistent results. Comparative genomics placed the strain within the *B. pacificus* group, with matching genome size and GC content across both platforms. We microencapsulated semi-purified extracellular proteases with maltodextrin and Arabic gum, then tested them in BALB/c mice as a model of carrageenan-induced thrombosis. Microencapsulation was intended to improve stability and enabled oral delivery of extracellular proteases while preserving their functional activity in a carrageenan-induced thrombosis model, which served as a biological validation system. Statistical analysis indicated selective modulation of intrinsic coagulation parameters without broad anticoagulant effects. These findings demonstrate how genome-guided enzyme discovery, combined with formulation engineering, can support the functional characterization of microbial proteases with potential applications in biotechnology and in enzyme stabilization strategies.

1. Introduction

Discovery and stabilization of functional microbial enzymes remain significant challenges in molecular biotechnology. This is particularly true when the aim is to convert protease diversity in genomes into reliable biocatalytic systems. Even though whole-genome sequencing has improved rapidly, there remains a gap between predicting protease types and confirming their effectiveness. This study aims to fill that gap by integrating genomic analysis and formulation engineering to study microencapsulated fibrinolytic proteases from *Bacillus pacificus* HSFI-5.

Thrombosis is a key factor in many serious cardiovascular diseases. While anticoagulant and thrombolytic treatments are commonly used to reduce the risk of stroke and heart attack, long-term use may increase the risk of bleeding (Afriansyah & Ethica, 2023). There is growing interest in using microbial fibrinolytic enzymes for controlled fibrin breakdown and other enzyme-based uses. One promising research avenue today is to identify enzymes in microorganisms, especially bacteria, with fibrin-degrading capabilities and potential applicability in enzyme-based biotechnological systems (Akhtar et al., 2017). Studies show that bacteria could be a valuable source of fibrinolytic proteases for both medical and biotechnological purposes (Fuad et al., 2020; Shettar et al., 2025).

Marine-derived *Bacillus* species represent an essential source of biotechnologically relevant extracellular enzymes, particularly fibrinolytic proteases with potential biotechnological applications. Earlier research has shown that fibrinolytic proteases from Bacillus species found with sea cucumbers have thrombolytic activity (Ayanti et al., 2022; Hidayati et al., 2021). One of them, *Bacillus pacificus* HSFI-5, was taken from the intestine of the fermented sea cucumber *Holothuria scabra and* produced crude protease extracts

with fibrinolytic activity. Previously, this strain was identified as *Bacillus tequilensis* by 16S rRNA gene sequencing using the Sanger method (Hidayati et al., 2021). Its crude proteolytic enzymes can break down blood clots by up to 68.2%, which matches or even surpasses commercial proteases such as Nattokinase (63.2%) (Hidayati et al., 2021). The wide range of potential uses for these proteases underscores their value in biotechnology and emphasizes the need to study the genome of the producing bacterium using whole-genome sequencing (WGS). WGS provides a comprehensive genetic map, helping researchers identify genes linked to enzyme activity, metabolic pathways, and potential therapeutic uses (Zhao et al., 2023).

Beyond therapeutic interest, fibrinolytic proteases represent valuable microbial biocatalysts with applications in industrial biotechnology, including protein processing, waste biotransformation, and functional enzyme development. Linking genome-derived enzyme prediction with experimentally validated activity remains a key challenge in microbial biotechnology. Therefore, integrating comparative genomics with formulation-based stabilization approaches provides an important framework for translating microbial enzyme diversity into usable biotechnological systems.

This study integrates genomic analysis of the fibrinolytic protease-producing strain HSFI-5 and *in vivo* assays of its microencapsulated, partly purified protease extract. The aim is to assess the biotechnological potential of HSFI-5 fibrinolytic proteases by combining genomic and functional validation methods. This research situates microbial fibrinolytic proteases within a molecular biotechnology context by integrating genome-based enzyme discovery, formulation engineering, and functional validation.

2. Materials and Methods

2.1. Sample Collection and Bacterial Culture

B. pacificus HSFI-5 (formerly reported as *B. tequilensis* HSFI-5) was used in this study. Its culture was obtained from the Microbiology Laboratory at Universitas Muhammadiyah Semarang, Indonesia. Bacterial colonies were rejuvenated in NB medium, and colony morphology was assessed by Gram staining and microscopy (Hidayati et al., 2021; Dewi et al., 2023).

2.2. DNA Extraction and Whole Genome Sequencing (WGS)

A standard bacterial DNA extraction kit (Qiagen Genomic DNA Kit, including Proteinase K treatment) was used to obtain high-quality genomic DNA suitable for WGS (Yang et al., 2023; Bearzatto et al., 2025). DNA quality and quantity using a NanoDrop spectrophotometer and gel electrophoresis. To obtain high-coverage whole-genome sequence data for strain HSFI-5, short-read WGS was performed on the Illumina and MGI platforms at PT Genetika Science Indonesia. For Illumina WGS, TruSeq library preparation kits were used, and sequencing was performed on a HiSeq to generate short reads (Gladkikh et al., 2023). For MGI, the DNBSEQ library preparation kit was used for high-throughput sequencing, which is suitable

for large-scale whole-genome sequencing. Sequencing was subsequently done on MGISEQ-2000 to generate short reads (Meslier et al., 2023; Hu et al., 2024; Zielińska et al., 2025).

2.3. WGS Data Analysis: Assembly and Annotation

Raw sequencing data from Illumina and MGI platforms were collected in the Galaxy Australia workspace. Trimmomatic or FastQC was used to remove low-quality reads, adapters, and contaminant sequences for trimming and quality filtering. De novo genome assembly was conducted using SPAdes (for Illumina reads) or ABySS (for MGI reads) (Jeon et al., 2023; Garcia-Fernandez et al., 2024). The quality of the assemblies was assessed using the N50 metric, while genome completeness and GC content were evaluated using BUSCO (Wang et al., 2023; Jeon et al., 2023). FASTA files generated by the data assembly process on the Illumina and MGI platforms were annotated with Prokka to identify the genome and predict genes (Zhao et al., 2025).

2.4. Taxonomic Identification

Taxonomic analysis of annotated data was performed using Kraken2, comparing the assembled genome to known bacterial databases (NCBI RefSeq and GTDB). The taxonomic identification results derived from the Illumina and MGI datasets were compared for cross-platform validation (Liu et al., 2024; Feng et al., 2024; Yarmosh et al., 2024).

2.5. Protease Coding Gene Identification

Prokka and RastK were used to annotate genes in the assembled genome (Gaba et al., 2022). The Search for the protease-coding genes was conducted using PATRIC, a resource of the Bacterial and Viral Bioinformatics Resource Center (BV-BRC). BLASTp or Pfam was used to compare predicted proteins with known protease databases. Further annotation of the bacterial genome was conducted using InterProScan to identify functional domains within the *vpr* gene and associated protease pathways (Olson et al., 2023; Lobb et al., 2023). Cross-referencing was performed against known protease family databases, such as MEROPS, to classify protease activity (Gerapati et al., 2025). The step is necessary to understand the protease's role in fibrinolysis and its potential applications.

2.6. Comparative Analysis of Taxonomic and Genomic Results

The comparative analysis evaluated the consistency of taxonomic and genomic results from Illumina and MGI sequencing platforms. Sequence quality between the two platforms was compared, and genome completeness was tested using QUAST. Core genome analysis and the average nucleotide identity (ANI) were calculated to evaluate taxonomic consistency (Sharma et al., 2023; Hu et al., 2024).

2.7. Data Integration, Visualization, and Interpretation

Illumina and MGI results were integrated using MultiQC to visualize sequencing data quality and platform-specific differences (Zhao et al., 2023). Proksee was also used to visualize bacterial genome

sequences from the Illumina and MGI platforms, showing genome coverage and protease gene locations (Grant et al., 2023).

2.8. Production of Semipurified Extract of Extracellular Fibrinolytic Proteases

Crude fibrinolytic protease from *B. pacificus* HSFI-5 was obtained by aerobic fermentation and recovery of the extracellular enzyme-rich supernatant, followed by confirmation of proteolytic and fibrinolytic activity using casein hydrolysis and fibrin plate assays. The crude extract was subsequently fractionated by ammonium sulfate precipitation and dialysis to enrich protease content while retaining multiple active components, as commonly applied for *Bacillus*-derived fibrinolytic enzymes (Astrup & Müllertz, 1952; Peng et al., 2005).

2.9. Microencapsulation of Protease Extract

Microencapsulation was applied as a stabilization strategy to preserve enzyme activity during downstream handling and to evaluate formulation-dependent functional performance of microbial proteases. The crude fibrinolytic protease from *B. pacificus* HSFI-5 was microencapsulated by spray drying using maltodextrin and Arabic gum (5% w/v each). The encapsulants were dissolved in crude enzyme solution and spray-dried at an inlet temperature of 110–180°C, outlet temperature of 60–70°C, and feed rate of 5–7 mL min^{-1}, as previously optimized (Weng et al., 2024).

2.10. In *vivo* Assays

The in vivo assay was used as a functional biological readout to assess whether genome-identified protease systems retained activity after formulation and stabilization.

2.10.1. Experimental Animals and Study Design

In vivo functional bioactivity was validated in male BALB/c mice (n = 30) acclimatized under standard laboratory conditions with free access to food and water (Dewi et al., 2023). Animals were randomly assigned to five experimental groups (n = 6 per group): a normal control group and four treatment groups receiving microencapsulated fibrinolytic protease formulations. The treatment groups consisted of maltodextrin-encapsulated protease at 150 mg/kg body weight (BW) (T1) and 200 mg/kg BW (T2), and Arabic gum-encapsulated protease at 150 mg/kg BW (T3) and 200 mg/kg BW (T4). Protease formulations were administered orally once daily. All experimental procedures were approved by the institutional ethics committee and conducted in accordance with applicable animal welfare guidelines (Nastiti et al., 2024).

2.10.2. Carrageenan-Induced Thrombosis Model

Experimental thrombosis was induced using a carrageenan-induced tail thrombosis model (Majumdar et al., 2016). Briefly, carrageenan solution was administered to induce localized inflammation and thrombus formation in the tail vasculature as previously described. This model was selected for its

reproducibility in assessing thrombolytic and antithrombotic activity via infarct length measurement and coagulation profiling (Dewi et al., 2023).

2.10.3. Body Weight Monitoring and General Toxicity Assessment

The body weight of each mouse was recorded weekly throughout the experimental period to monitor general health status and potential systemic toxicity. Changes in body weight were used as an indicator of treatment tolerability and overall physiological impact of the fibrinolytic protease formulations (Majumdar et al., 2016).

2.10.4. Measurement of Thrombus Infarct Length

Thrombus formation was evaluated by measuring tail infarct length at 48 h following carrageenan induction. The 48-hour post-induction time point was selected for primary infarct analysis and visual documentation, as it represents a stabilized thrombotic phase with reduced acute inflammatory variability compared to earlier time points. Infarct length was defined as the visibly necrotic or ischemic segment of the tail and was measured using a calibrated ruler. The infarct length served as a macroscopic indicator of thrombotic severity and thrombolytic efficacy (Majumdar et al., 2016; Dewi et al., 2023).

2.10.5. Prothrombin Time (PT) and Activated Partial Thromboplastin Time (aPTT) Assay

Animal blood samples were collected at three time points: before treatment (baseline), 24 h, and 28 h after treatment administration. Prothrombin time (PT) was measured in seconds using standard coagulation assay procedures to assess modulation of the extrinsic coagulation pathway. PT values were recorded for each animal and expressed as mean ± standard deviation (SD) for each experimental group. Activated partial thromboplastin time (aPTT) was determined from plasma samples collected at the same time points as PT analysis. The aPTT assay was used to evaluate effects on the intrinsic coagulation pathway. Results were expressed as mean ± SD for each group (Dewi et al., 2023; Ethica et al., 2023).

2.10.6. Plasma D-Dimer Measurement

Plasma D-dimer levels were quantified following carrageenan-induced thrombosis to assess fibrin degradation activity. Blood samples were centrifuged to obtain plasma, and D-dimer concentrations were measured using a commercially available ELISA kit according to the manufacturer's instructions. Elevated D-dimer levels were interpreted as an indicator of enhanced fibrinolytic activity (Reda et al., 2022).

3. Results

3.1. Bacterial Rejuvenation and Phenotypic Confirmation

HSFI-5 bacterial cells were rejuvenated in nutrient broth (NB) medium at 37 °C under shaking conditions. The culture exhibited stable growth characteristics consistent with previous observations (see supplementary files). Microscopic examination following Gram staining revealed Gram-positive, rod-shaped bacterial cells, in agreement with the phenotypic features previously reported for this strain. In addition, HSFI-5 demonstrated extracellular protease activity, as confirmed by qualitative protease assays (Hidayati et al., 2021). These phenotypic characteristics are consistent with earlier reports on *B. tequilensis* HSFI-5, confirming strain identity and functional stability before downstream genomic and *in vivo* analyses.

3.2. Genomic Analysis

3.2.1. Quality and Coverage of Sequencing Data

The FastQC results confirm that the Illumina sequencing data are of high quality, with sufficient base accuracy, balanced GC content, and minimal technical bias (as summarized in Supplementary Figure S1). These characteristics support the reliability of subsequent *de novo* genome assembly, taxonomic analysis, and protease gene identification.

3.2.2. Genome Assembly and Annotation

Comparative results of bacterial genome assembly and annotation of *B. pacificus* HSFI-5 using Illumina and MGI are displayed in **Table 1**. The GC content was highly similar across assemblies (35.29% for Illumina and 35.39% for MGI), implying minimal platform-specific GC bias and a stable base composition. In terms of assembly contiguity, the Illumina dataset yielded 120 contigs, whereas the MGI dataset produced 140 contigs, suggesting a slightly higher level of fragmentation in the MGI assembly.

As seen in Table 1, the longest contig length obtained from the Illumina assembly was 317,253 bp, compared with 275,301 bp for the MGI assembly. This difference shows that the Illumina data provided slightly better long-range continuity, likely due to more uniform per-base sequencing quality. The shortest contig lengths were 130,085 bp (Illumina) and 104,610 bp (MGI), reflecting differences in assembly resolution at low-coverage or repetitive regions.

Table 1. Genome assembly and annotation of *B. pacificus* HSFI-5 using Illumina and MGI

Assembly Parameters	Values	
	Illumina	MGI
Genome size (bp)	5,452,325	5,482,348
GC content (%)	35.29	35.39
Number of contigs	120	140
Longest contig	317,253	275,301
Shortest contig	130	104

Overall, the Illumina assembly exhibited slightly higher contiguity. In contrast, the MGI assembly provided comparable genome completeness, supporting the complementary use of both datasets to enhance confidence in genomic characterization of *Bacillus pacificus* HSFI-5. Illumina data yielded fewer contigs and longer maximum contig length, indicating slightly higher assembly contiguity, while MGI data provided comparable genome completeness suitable for downstream genomic analyses.

3.2.3. Taxonomic Classification and Identification of Protease-Coding Genes

Genomic analysis placed strain HSFI-5 within the *Bacillus pacificus* clade, showing close phylogenetic relatedness to reference *B. pacificus* genomes **(Figure 1)**. This placement differs from its earlier identification as *B. tequilensis* based on 16S rRNA sequencing.

Data from PATRIC were curated, and proteases of *B. pacificus* HSFI-5 were grouped according to their direct or indirect involvement in fibrin degradation and extracellular enzyme deployment (**Table 2**). Consistent with data in Figure 1B, the protease profile of *B. pacificus* HSFI-5 shows a coordinated system that supports fibrin-degrading functional activity (Table 2). *Vpr*, a subtilisin-like extracellular serine protease, gives a clear genomic basis for fibrinolytic activity by breaking down fibrin in a way similar to plasmin. The gene shows homology to minor extracellular serine proteases reported in the *Bacillus subtilis* species complex, indicating a conserved fibrinolytic role. Other extracellular serine proteases and metalloproteases may also help remodel fibrin. Signal peptidases and regulatory proteases help with the secretion, maturation, and stability of these enzymes. Together, this provides a genomic framework consistent with the observed fibrinolytic activity, although direct enzyme-specific validation remains necessary

Table 2. Protease-encoding genes identified in the *B. pacificus* HSFI-5 genome with potential roles in antithrombotic and fibrinolytic activity (see Supplementary PATRIC table data).

No.	Gene	Protease	Protease Class & position (bp)	Biological Function	Role in Antithrombotic Activity
1	*vpr*	Vpr (minor extracellular protease)	Serine protease (2776496-2779249)	Extracellular protein degradation	Direct fibrinolytic activity; plasmin-like or fibrin-degrading potential
2	*aprE*	Extracellular alkaline serine protease (subtilase family)	Serine protease (933846 932653)	Protein and peptide hydrolysis	Likely contributes to fibrinolysis in the extracellular environment
3	*inhA*	Immune inhibitor A	Metalloprotease (Zn-dependent) (1483556 1481172)	Broad extracellular proteolysis	Indirect fibrin degradation through non-specific proteolysis
4	*sipW*	Signal peptidase I (SipW)	Signal peptidase (1545208 1544687)	Cleavage of signal peptides	Enables secretion of extracellular fibrinolytic proteases
5	*pepF*	Oligoendopeptidase F	Cytosolic peptidase (1882159 1883946)	Peptide turnover and regulation	Supports protease maturation and activity balance
6	*comC*	Competence-associated protease (ComC)	Processing protease (52672-53394)	Peptide signalling	Regulatory support of protease expression
7	*clpCP* / *mecA*	ClpP protease adaptor proteins	Protein quality control (214220-214828)	Protease folding and stability	Maintains functional protease systems

The identification of multiple extracellular serine protease and metalloprotease genes reflects a coordinated enzymatic system that contributes to fibrin degradation rather than relying on a single catalytic protein. This genome-informed interpretation provides a mechanistic framework linking gene repertoire to the observed fibrinolytic bioactivity.

3.3. Microencapsulation of bacterial crude fibrinolytic protease

To ensure reliable oral administration and functional *in vivo* assessment, we formulated the fibrinolytic protease extract using a microencapsulation approach. Microencapsulation of the semipurified fibrinolytic protease extract from *B. pacificus* HSFI-5 was successfully achieved by spray drying with maltodextrin and Arabic gum as encapsulating agents, each at 5% relative to the crude protease extract

(**Figure 2**). The spray-drying process produced a fine, free-flowing powder with no visible aggregation, indicating effective encapsulation and efficient drying.

The resulting microencapsulated protease exhibited good physical stability and was readily reconstituted for subsequent *in vivo* administration. The use of a combined maltodextrin and Arabic gum formulation as a wall material yielded a formulation suitable for oral dosing, supporting consistent handling and dosing accuracy during animal experiments. Notably, the encapsulated protease retained its biological activity, as evidenced by its ability to modulate coagulation parameters, reduce thrombus infarct length, and modulate plasma D-dimer levels in treated animals.

3.4. In *Vivo* Thrombolysis Activity Assays

The collected *in vivo* data were used to assess changes in coagulation parameters, thrombus formation, and fibrinolytic activity following administration of the microencapsulated protease. All statistical analysis was performed using one-way ANOVA followed by Tukey's multiple comparison test. Data are presented as mean ± standard deviation. Differences were considered statistically significant at $p < 0.05$.

Body weight measurements (Table 1) demonstrated relative stability across all experimental groups over the two-week observation period. The normal control group showed a modest increase in mean body weight from Week 1 to Week 2, consistent with normal physiological growth. In protease-treated groups, both microencapsulated (M) and Arabic gum (AG) formulations exhibited minor fluctuations in body weight; however, no progressive or dose-dependent weight loss was observed, including at the highest dose of 200 mg/kg BW.

Table 3. Body Weight of Mice During the Experimental Period (Mean ± SD)

Treatment Group	Body Weight (g)	
	Week 1	Week 2
Normal Control	21.53 ± 1.62	22.93 ± 1.15
T1 – M 150 mg/kg BW	23.93 ± 0.86	23.43 ± 0.93
T2 – M 200 mg/kg BW	26.03 ± 2.05	25.98 ± 1.68
T3 – AG 150 mg/kg BW	24.83 ± 2.16	23.82 ± 1.35
T4 – AG 200 mg/kg BW	26.07 ± 2.05	25.03 ± 1.86

Abbreviations: M = Maltodextrin encapsulated fibrinolytic protease; AG = Arabic gum encapsulated fibrinolytic protease; BW = body weight. Data are presented as mean ± SD (n = 6 per group).

Notably, variability within treatment groups (SD range: 0.86–2.16 g at Week 1 and 0.93–1.86 g at Week 2) remained within expected physiological limits for BALB/c mice. These results indicate that administration of the fibrinolytic protease formulations was well tolerated, with no apparent adverse effects on general systemic health during the experimental period.

Measurement of tail infarct length revealed variability among individual animals across all experimental groups (Figure 3). Although several treated groups showed numerically shorter infarct segments compared with the control group, one-way ANOVA analysis indicated that these differences were not statistically significant (F = 2.08, p = 0.114).

The observed dispersion reflects the inherent biological variability of the carrageenan-induced thrombosis model, in which inflammatory responses and vascular sensitivity differ among animals. Therefore, while visual trends suggest a possible reduction in thrombus severity following protease administration (Figure 4), the present data do not demonstrate a statistically confirmed treatment effect under the tested conditions.

Prothrombin time values showed gradual convergence among groups during the observation period (Table 4). Despite minor fluctuations between treatments, statistical analysis demonstrated no significant differences among experimental groups (one-way ANOVA, F = 0.20, p = 0.934).

Table 4. Prothrombin Time (PT) in BALB/c Mice (Mean ± SD)

Treatment Group	PT (s) – Pre-treatment	PT (s) – 24 h	PT (s) – 48 h
Normal Control	36.83 ± 8.91	23.67 ± 2.42	17.50 ± 4.97
T1 – M 150 mg/kg BW	25.00 ± 3.29	20.67 ± 3.27	16.33 ± 3.01
T2 – M 200 mg/kg BW	26.00 ± 5.22	19.17 ± 2.32	16.67 ± 0.52
T3 – AG 150 mg/kg BW	21.33 ± 5.47	31.67 ± 12.11	16.17 ± 2.04
T4 – AG 200 mg/kg BW	22.83 ± 2.04	21.17 ± 3.13	17.00 ± 2.00

Abbreviations: aPTT = activated partial thromboplastin time; s = seconds; M = maltodextrin encapsulated fibrinolytic protease; AG = Arabic gum encapsulated fibrinolytic protease; BW = body weight.
Data are presented as mean ± standard deviation (n = 6 per group), analysis performed using one-way ANOVA (F value = 0.20 and p value = 0.934)

These results indicate that oral administration of the microencapsulated protease formulations did not produce measurable alterations in the extrinsic coagulation pathway. The reduction in variability observed at later time points likely reflects physiological stabilization following carrageenan induction rather than a treatment-specific anticoagulant effect.

In contrast to PT measurements, activated partial thromboplastin time (aPTT) differed significantly among experimental groups (one-way ANOVA, F = 4.82, p = 0.005) (Table 5). A progressive reduction in aPTT values was observed at 48 h in several treatment groups, particularly in animals receiving the higher protease doses (T2 and T4).

Table 5. Activated Partial Thromboplastin Time (aPTT) in BALB/c Mice (Mean ± SD)

Treatment Group	aPTT (s) – Pre-treatment	aPTT (s) – 24 h	aPTT (s) – 48 h
Normal Control	64.67 ± 11.11	66.67 ± 7.15	42.00 ± 9.86
T1 – M 150 mg/kg BW	53.00 ± 10.88	50.00 ± 16.26	33.83 ± 2.99
T2 – M 200 mg/kg BW	78.00 ± 14.06	60.00 ± 11.17	32.67 ± 9.91
T3 – AG 150 mg/kg BW	55.17 ± 17.59	44.33 ± 8.21	33.83 ± 2.48
T4 – AG 200 mg/kg BW	51.17 ± 16.95	62.33 ± 15.19	23.17 ± 5.98

Abbreviations: aPTT = activated partial thromboplastin time; s = seconds; M = maltodextrin encapsulated fibrinolytic protease; AG = Arabic gum encapsulated fibrinolytic protease; BW = body weight.
Data are presented as mean ± standard deviation (n = 6 per group), analysis performed using one-way ANOVA (F value = 4.82 and p value = 0.005)

As seen in **Table 5**, post-treatment convergence toward lower aPTT values suggests modulation of intrinsic coagulation dynamics following protease administration. Because baseline variability was present before treatment, these findings should be interpreted as treatment-associated modulation rather than absolute anticoagulant activity.

Figure 5 shows that plasma D-dimer levels varied between treatment groups following carrageenan-induced thrombosis. Although differences in mean values were observed, statistical analysis did not demonstrate significant group separation (one-way ANOVA, F = 2.42, p = 0.094).

Data are presented as mean ± standard deviation (n = 6 per group), analysis performed using one-way ANOVA (F value = 2.42 and p value = 0.094)

The pattern in Figure 5, therefore, suggests a tendency toward altered fibrin turnover rather than a statistically confirmed increase in fibrinolytic activity. Because D-dimer concentrations reflect the balance between clot formation and degradation, these variations may represent temporal differences in thrombus resolution rather than differences in overall enzymatic potency.

Differences between maltodextrin and Arabic gum formulations may reflect variations in enzyme availability following administration. Because release kinetics were not directly measured, these interpretations remain hypothetical and require dedicated release studies for confirmation. Because D-dimer levels depend on both fibrin formation and fibrin degradation, reduced levels at later time points may reflect decreased thrombus burden rather than reduced fibrinolytic activity.

The differences in D-dimer responses between maltodextrin (M) and Arabic gum (AG) microcapsule formulations imply that the microcarrier type may affect the timing of fibrin turnover after treatment.

However, this study did not directly measure the rate of enzyme release. In general, groups treated with M showed lower D-dimer levels at 48 hours compared to those treated with AG. Because D-dimer reflects the balance between fibrin formation and breakdown, lower levels at this point may indicate less thrombus or earlier fibrinolysis, not that the treatment was less active.

On the other hand, higher D-dimer levels in AG-treated groups, especially at higher doses, suggest that fibrin was still being degraded at the time samples were collected. These differences may be due to the physical and chemical properties of the materials used to make the microcapsules. Arabic gum creates more complex networks that can affect how enzymes are released and how stable they are, while maltodextrin usually dissolves faster.

Since the study did not directly measure release or pharmacokinetics, any conclusions about the mechanism should be made cautiously. Looking at infarct outcomes and blood clotting measures, both types of capsules seem to affect the balance between clotting and fibrinolysis, probably by altering the timing of their effects rather than their overall effectiveness. More in-depth research is needed to understand how the enzymes are released, how long they persist in the body, and how the capsule materials influence these outcomes.

4. Discussion

The present study integrates microbial genomics, enzyme production, and formulation engineering to evaluate functional properties of extracellular proteases produced by Bacillus pacificus HSFI-5. Rather than assessing therapeutic efficacy, the carrageenan-induced thrombosis model was used as a biological system to verify preservation of fibrinolytic functionality following microencapsulation.

Whole-genome sequencing of strain HSFI-5 followed by *in vivo* thrombosis assays was performed to evaluate how fibrinolytic proteases from *B. pacificus* HSFI-5 affect blood clotting. The results suggest that the proteases encoded by these genes are consistent with the fibrinolytic activity observed experimentally. This indicates functional fibrin-degrading capability consistent with potential enzyme biotechnology applications.

Whole-genome analysis using the Illumina and MGI platforms yielded similar results for genome size and GC content, indicating that the genome was sequenced reliably with minimum platform bias. Slight discrepancies in contig number and length were expected due to the sequencing and assembly methods. Both datasets consistently placed HSFI-5 within the *Bacillus pacificus* lineage, despite minor reference-dependent variation inherent to short-read assemblies. This finding was expected and does not affect the main conclusions. Genome annotation identified fibrinolytic protease genes, including *vpr*, which are likely involved in the observed fibrinolytic bioactivity.

Spray drying with maltodextrin and Arabic gum (5% each) successfully produced a microencapsulated protease preparation that enabled consistent handling during *in vivo* evaluation, with preserved biological activity demonstrated in subsequent *in vivo* assays. Tests using the carrageenan-induced

thrombosis model showed that the protease specifically affects blood clotting pathways. The carrageenan-induced thrombosis model was employed as a functional bioactivity assay, serving as a controlled system for evaluating fibrinolytic enzyme performance under physiological conditions.

Functional evaluation in the carrageenan-induced thrombosis model revealed selective effects on coagulation parameters. Statistical analysis indicated no significant differences in PT values or infarct length among treatment groups, suggesting that the formulations did not exert a broad anticoagulant or thrombolytic effect under the experimental conditions. Tukey's post hoc analysis indicated that groups T2 and T4 differed significantly from the control group ($p < 0.05$), whereas other comparisons were not significant. The relatively small group size ($n = 6$) may have limited statistical power to detect moderate treatment effects, which could explain the presence of biological trends that did not reach statistical significance.

In contrast, significant differences detected in aPTT measurements indicate that the protease preparations may influence components of the intrinsic coagulation pathway. This selective modulation is consistent with controlled fibrin turnover rather than systemic coagulation suppression. The reduction in aPTT may reflect indirect modulation of inflammatory coagulation dynamics rather than classical anticoagulant activity, a phenomenon previously observed in inflammation-driven thrombosis models. Carrageenan-induced thrombosis involves inflammatory coagulation activation, and modulation of this process may normalize clotting dynamics rather than produce classical anticoagulant prolongation. Variations in infarct size and D-dimer profiles should therefore be interpreted cautiously, as these outcomes showed trends rather than statistical significance. Such patterns may reflect biological heterogeneity inherent to inflammation-driven thrombosis models rather than direct dose-dependent enzymatic effects.

In comparison, maltodextrin-based formulations had infarct sizes similar to those of the negative control, indicating little effect. The weaker results at higher Arabic gum doses are likely due to slower enzyme release, since higher viscosity can limit how well the enzyme spreads and is absorbed, which is a common problem with encapsulated enzymes. The combined results from genome data, D-dimer levels, clotting tests, and infarct measurements show a biologically consistent relationship between the genomic protease repertoire and observed functional trends.

In contrast to the earlier study by Dewi et al. (2023), which used injected bacterial crude protease extracts directly to the tail, this research tested the oral use of microencapsulated protease. This method better reflects a clinically relevant way to deliver the enzyme, helps prevent degradation, and keeps its fibrinolytic activity in the body. These findings indicate that HSFI-5 protease represents a microbial fibrinolytic enzyme system warranting further biological investigation.

Instead of acting as a general anticoagulant, the *B. pacificus* HSFI-5 protease appears to support controlled fibrinolysis, which may lower the risk of clots while maintaining normal blood clotting. Because of natural differences in the model and small sample sizes, nonparametric statistics and detailed data visualization were used to obtain accurate results.

Taken together, the genomic identification of multiple extracellular protease genes provides a mechanistic framework for fibrin degradation, while *in vivo* findings demonstrate physiological compatibility and selective modulation of coagulation. Rather than indicating definitive thrombolytic efficacy, the present results establish the functional plausibility of linking genomic enzyme repertoires to measurable biological responses.

Identification of multiple protease genes, together with modulation of PT/aPTT values and treatment-dependent changes in D-dimer profiles, is consistent with biological trends suggestive of fibrinolytic activity, although statistical confirmation was limited. Using comparative genomics and *in vivo* testing links enzyme gene profiles to observed fibrin-degrading activity in different microbes. The results show that microencapsulated proteases can be stable biocatalysts and help develop enzyme-based technologies for controlled fibrin modulation, guided by genomic data.

Overall, the oral microencapsulated protease showed preliminary *in vivo* compatibility and selective effects on coagulation parameters, with trends suggestive of biological activity that did not reach statistical significance. These results support further optimization and validation through studies with larger datasets and improved statistical power to better define functional performance and potential biotechnological applications.

Future studies should examine how the protease is processed in vivo, its long-term safety, its comparison with other fibrinolytic enzyme systems, and ways to improve bioprocessing and formulation. Together, these results create a genome-based framework that connects microbial protease diversity, formulation engineering, and bioactivity testing, supporting future studies exploring biological and biochemical characteristics of microbial fibrinolytic enzymes.

5. Conclusions

This study demonstrates that genome-informed analysis, combined with formulation engineering, provides an effective strategy for the functional characterization of microbial protease systems. Genomic identification of fibrinolytic protease genes guided functional evaluation, while in vivo assays confirmed preservation of fibrinolytic activity following microencapsulation. While statistical significance was primarily observed in aPTT modulation, trends in thrombus-related parameters suggest that formulation optimization and release kinetics warrant further investigation. The integration of comparative genomics, enzyme stabilization, and functional testing establishes a framework for developing microbial proteases as robust biotechnological tools.

Declarations

Conflict of Interest:

The authors declare no conflict of interest.

Ethical Approval:

Approved by the Health Research Ethics Commission, Faculty of Public Health, Universitas Muhammadiyah Semarang, Indonesia (Approval No. 377/KEPK-FKM/UNIMUS/2020).

Funding

This work was supported by the Ministry of Education, Culture, Research, and Technology of the Republic of Indonesia through the Applied Research Grant Program (Hibah Penelitian Terapan), fiscal years 2023–2024 (Grant No. 022/061026/PB/SP2H/AK04/2024).

Author Contribution

SNE led the project and manuscript preparation. YSP and WH performed genome assembly and bioinformatics analyses. DSZ conducted microencapsulation experiments. MDL and SR carried out animal studies and statistical analyses. ST assisted with bacterial culture and gene analysis. TM reviewed the data analysis and critically checked the manuscript.

Acknowledgements

The authors gratefully acknowledge the Fulbright Program for facilitating international research networking, and LPPT Universitas Gadjah Mada and PT Genetika Science Indonesia for their technical support.

Data Availability

The datasets generated during and/or analysed during the current study are available from the corresponding author on reasonable request.

References

1. Afriansyah MA, Ethica SN (2023) Fibrinolytic Protease-Producing Bacteria with Varied Hemolysis Pattern Associated with Marine Algae Dictyota sp. Med Lab Technol J 9(2). https://doi.org/10.31964/mltj.v9i2.525
2. Akhtar T, Hoq MM, Mazid MA (2017) Bacterial proteases as thrombolytics and fibrinolytics. Dhaka Univ J Pharm Sci 16(2):255–269. https://doi.org/10.3329/dujps.v16i2.35265
3. Altaf F, Wu S, Kasim V (2021) Role of fibrinolytic enzymes in anti-thrombosis therapy. Front Mol Biosci 8:680397. https://doi.org/10.3389/fmolb.2021.680397

4. Astrup T, Müllertz S (1952) The fibrin plate method for estimating fibrinolytic activity. Arch Biochem Biophys 40(2):346–351. https://doi.org/10.1016/0003-9861(52)90121-5
5. Ayanti BP, Ethica SN, Sulisytaningtyas AR, Dewi SS, Zilda DS Prospective purification and assay of thrombolytic protease from Bacillus sp. hsfi-10 isolated from sand sea cucumber for antithrombotic agent development. In 7th International Conference on Biological Science (ICBS 2021), 2022 May 2 (pp. 404–415). Atlantis Press. https://doi.org/10.2991/absr.k.220406.057
6. Bearzatto B, Durant JF, Ambroise J, Gala JL (2025) Rapid, user-friendly, cost-effective DNA and library Preparation methods for whole-genome sequencing of bacteria with varying cell wall composition and GC content using minimal DNA on the Illumina platform. BMC Genomics 26(1):396. https://doi.org/10.1186/s12864-025-11598-7
7. Dewi OY, Zilda DS, Rakhmawatie MD, Samiasih A, Ethica SN (2023) In vivo antithrombotic potential of protease from Bacillus thuringiensis HSFI-12. Scripta Med 54(3):229–236. https://doi.org/10.5937/scriptamed54-44973
8. Ethica SN, Raharjo TJ, Zilda DS, Hidayati N (2023) In vitro anticoagulant activity of crude protease of Bacillus tequilensis HSFI-5. Indonesian J Med Lab Sci Technol 5(2):90–99. https://doi.org/10.33086/ijmlst.v5i2.3791
9. Feng Z, Peng F, Xie F, Liu Y, Zhang H, Ma J, Xing J, Guo X (2024) Comparison of capture-based mtDNA sequencing performance between MGI and Illumina sequencing platforms in various sample types. BMC Genomics 25(1):41. https://doi.org/10.1186/s12864-023-09938-6
10. Fuad H, Hidayati N, Darmawati S, Munandar H, Sulistyaningtyas AR, Nurrahman N, Ernanto AR, Zilda DS, Widjanarka W, Ethica SN Prospects of fibrinolytic proteases of bacteria from sea cucumber fermentation products as an antithrombotic agent. In BIO Web of Conferences 2020 (Vol. 28, p. 02006). EDP Sciences. https://doi.org/10.1051/bioconf/20202802006
11. Fuks G, Elgart M, Amir A, Zeisel A, Turnbaugh PJ, Soen Y, Shental N (2018) Combining 16S rRNA gene variable regions enables high-resolution microbial community profiling. Microbiome 6(1):17. https://doi.org/10.1186/s40168-017-0396-x
12. Gaba S, Naitam MG, Kumari A, Medema MH, Kaushik R (2022) Comprehensive Genome Analysis of Halolamina pelagica CDK2: Insights into Abiotic Stress Tolerance Genes. J Pure Appl Microbiol 16(1). https://doi.org/10.22207/JPAM.16.1.44
13. Garapati PV, Zaru R, Attrill H, Dos Santos G, Goodman J, Thurmond J, Marygold SJ (2025) Comprehensive annotation of the enzymes of Drosophila melanogaster. G3: Genes, Genomes, Genetics. Dec 8:jkaf294. https://doi.org/10.1093/g3journal/jkaf294
14. Garcia-Fernandez A, Janowicz A, Marotta F, Napoleoni M, Arena S, Primavilla S, Pitti M, Romantini R, Tomei F, Garofolo G, Villa L (2024) Antibiotic resistance, plasmids, and virulence-associated markers in human strains of *Campylobacter jejuni* and *Campylobacter coli* isolated in Italy. Front Microbiol 14:1293666. https://doi.org/10.3389/fmicb.2023.1293666
15. Gladkikh A, Klyuchnikova E, Pavlova P, Sbarzaglia V, Tsyganova N, Popova M, Arbuzova T, Sharova A, Ramsay E, Samoilov A, Dedkov V (2023) Comparative Analysis of Library Preparation Approaches

for SARS-CoV-2 Genome Sequencing on the Illumina MiSeq Platform. Int J Mol Sci 24(3):2374. https://doi.org/10.3390/ijms24032374

16. Grant JR, Enns E, Marinier E, Mandal A, Herman EK, Chen CY, Graham M, Van Domselaar G, Stothard P (2023) Proksee: in-depth characterization and visualization of bacterial genomes. Nucleic Acids Res 51(W1):W484–W492. https://doi.org/10.1093/nar/gkad326
17. Hidayati N, Nurrahman N, Fuad H, Munandar H, Zilda DS, Ernanto AR, Samiasih A, Oedjijono O, Ethica SN Bacillus tequilensis isolated from the fermented intestine of Holothuria scabra produces a fibrinolytic protease with thrombolytic activity. In IOP conference series: Earth and environmental science 2021 Mar 1 (Vol. 707, No. 1, p. 012008). IOP Publishing. https://iopscience.iop.org/article/10.1088/1755-1315/707/1/012008/pdf
18. Hu T, Chen J, Lin X, He W, Liang H, Wang M, Li W, Wu Z, Han M, Jin X, Kristiansen K (2024) Comparison of the DNBSEQ platform and Illumina HiSeq 2000 for bacterial genome assembly. Sci Rep 14(1):1292. https://doi.org/10.1038/s41598-024-51725-0
19. Jeon MS, Jeong DM, Doh H, Kang HA, Jung H, Eyun SI (2023) A practical comparison of the next-generation sequencing platform and assemblers using yeast genome. Life Sci Alliance 6(4). http://doi.org/10.26508/lsa.202201744
20. Liu Y, Ghaffari MH, Ma T, Tu Y (2024) Impact of database choice and confidence score on the performance of taxonomic classification using Kraken2. aBIOTECH 5(4):465–475. https://doi.org/10.1007/s42994-024-00178-0
21. Lobb B, Shapter A, Doxey AC, Nissimov JI (2023) Functional profiling and evolutionary analysis of a marine microalgal virus pangenome. Viruses 15(5):1116. https://doi.org/10.3390/v15051116
22. Majumdar S, Chattopadhyay P, Mukherjee AK (2016) In vivo anticoagulant and thrombolytic activities of a fibrinolytic serine protease (Brevithrombolase) with the k-carrageenan-induced rat tail thrombosis model. Clin Appl Thromb Hemost 22(6):594–598. https://doi.org/10.1177/1076029615569567
23. Meslier V, Quinquis B, Da Silva K, Plaza Oñate F, Pons N, Roume H, Podar M, Almeida M (2022) Benchmarking second and third-generation sequencing platforms for microbial metagenomics. Sci Data 9(1):694. https://doi.org/10.1038/s41597-022-01762-z
24. Nastiti HR, Ethica SN, Samiasih A, Saptaningtyas R, Zilda DS, Kamaruddin M, Mukaromah AH In vivo study using rat model to evaluate anti-thrombotic activity of protease from Bacillus cereus HSFI-10–A review. In AIP Conference Proceedings 2024 Mar 7 (Vol. 3080, No. 1, p. 130003). AIP Publishing LLC. https://doi.org/10.1063/5.0198540
25. Olson RD, Assaf R, Brettin T, Conrad N, Cucinell C, Davis JJ, Dempsey DM, Dickerman A, Dietrich EM, Kenyon RW, Kuscuoglu M (2023) Introducing the bacterial and viral bioinformatics resource center (BV-BRC): a resource combining PATRIC, IRD, and ViPR. Nucleic Acids Res 51(D1):D678–D689. https://doi.org/10.1093/nar/gkac1003
26. Peng Y, Huang Q, Zhang RH, Zhang YZ (2003) Purification and characterization of a fibrinolytic enzyme produced by Bacillus amyloliquefaciens DC-4 screened from douchi, a traditional Chinese

soybean food. Comp Biochem Physiol B: Biochem Mol Biol 134(1):45–52. https://doi.org/10.1016/S1096-4959(02)00183-5

27. Reda S, Thiele Serra E, Müller J, Hamedani NS, Oldenburg J, Pötzsch B, Rühl H (2022) Increased prevalence of elevated D-dimer levels in patients on direct oral anticoagulants: results of a large retrospective study. Front Cardiovasc Med 9:830010. https://doi.org/10.3389/fcvm.2022.830010
28. Satam H, Joshi K, Mangrolia U, Waghoo S, Zaidi G, Rawool S, Thakare RP, Banday S, Mishra AK, Das G, Malonia SK (2023) Next-generation sequencing technology: current trends and advancements. Biology 12(7):997. https://doi.org/10.3390/biology12070997
29. Sharma T, Kumar R, Kalra JS, Singh S, Bhalla GS, Bhardwaj A, Galaxy ASIST (2023) A web-based platform for mapping and assessment of global standards of antimicrobial susceptibility: A case study in Acinetobacter baumannii genomes. Front Microbiol 13:1041847. https://doi.org/10.3389/fmicb.2022.1041847
30. Shettar SS, Bagewadi ZK, Alasmary M, Mannasaheb BA, Shaikh IA, Khan AA (2025) Comprehensive biochemical, molecular, and structural characterization of subtilisin with fibrinolytic potential in bioprocessing. Bioresources Bioprocess 12(1):21. https://doi.org/10.1186/s40643-025-00860-1
31. Wang P, Wang F (2023) A proposed metric set for evaluation of genome assembly quality. Trends Genet 39(3):175–186. https://doi.org/10.1016/j.tig.2022.10.005
32. Weng Y, Li Y, Chen X, Song H, Zhao CX (2024) Encapsulation of enzymes in the food industry via spray drying: Recent advances and scale-up. Crit Rev Food Sci Nutr 64(22):7941–7958. https://doi.org/10.1080/10408398.2023.2193982
33. Yang J, Shang P, Zhang B, Wang J, Du Z, Wang S, Xing J, Zhang H (2023) Genomic and metabonomic methods reveal the probiotic functions of swine-derived Lactobacillus salivarius. BMC Microbiol 23(1):242. https://doi.org/10.1186/s12866-023-02993-9
34. Yarmosh DA, Lopera JG, Puthuveetil NP, Combs PF, Reese AL, Tabron C, Pierola AE, Duncan J, Greenfield SR, Marlow R, King S (2022) Comparative analysis and data provenance for 1,113 bacterial genome assemblies. Msphere 7(3):e00077–e00022. https://doi.org/10.1128/msphere.00077-22
35. Zhao C, Zhang Z, Sun L, Bai R, Wang L, Chen S (2023) Genome sequencing provides potential strategies for drug discovery and synthesis. Acupunct Herb Med 3(4):244–255. https://doi.org/10.1097/HM9.0000000000000076
36. Zhao Y, Olsen JE, Poulsen L, Christensen H Comparison of genomic assembly and annotation based on two clones of avian pathogenic Escherichia coli. Res Microbiol 2025 Sep 29:104345. https://doi.org/10.1016/j.resmic.2025.104345
37. Zielińska K, Pantiukh K, Łabaj PP, Kosciolek T, Org E A large-scale comparative metagenomic analysis of short-read sequencing platforms indicates high taxonomic concordance but challenges in functional analysis. bioRxiv 2025 Jul 7:2025–2007. https://doi.org/10.1101/2025.07.06.662369

Figures

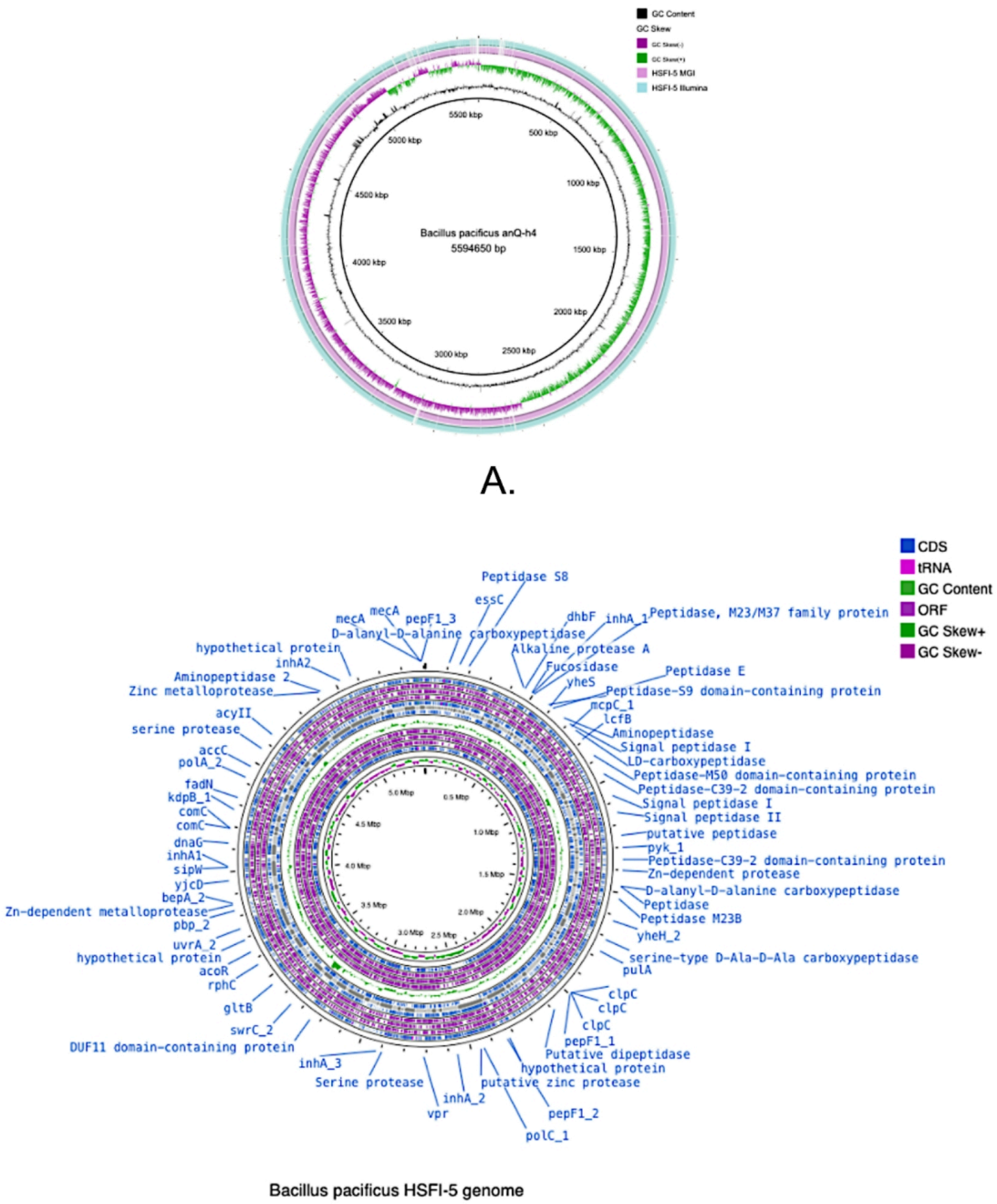


Figure 1

Visualization of *Bacillus pacificus* HSFI-5 genome. A. Circular genome of *Bacillus pacificus* HSFI-5 as a comparative coverage from both Illumina and MGI sequencing platforms; B. Proksee HSFI-5 bacterial genome visualization containing protease-encoding genes identified through genome annotation.

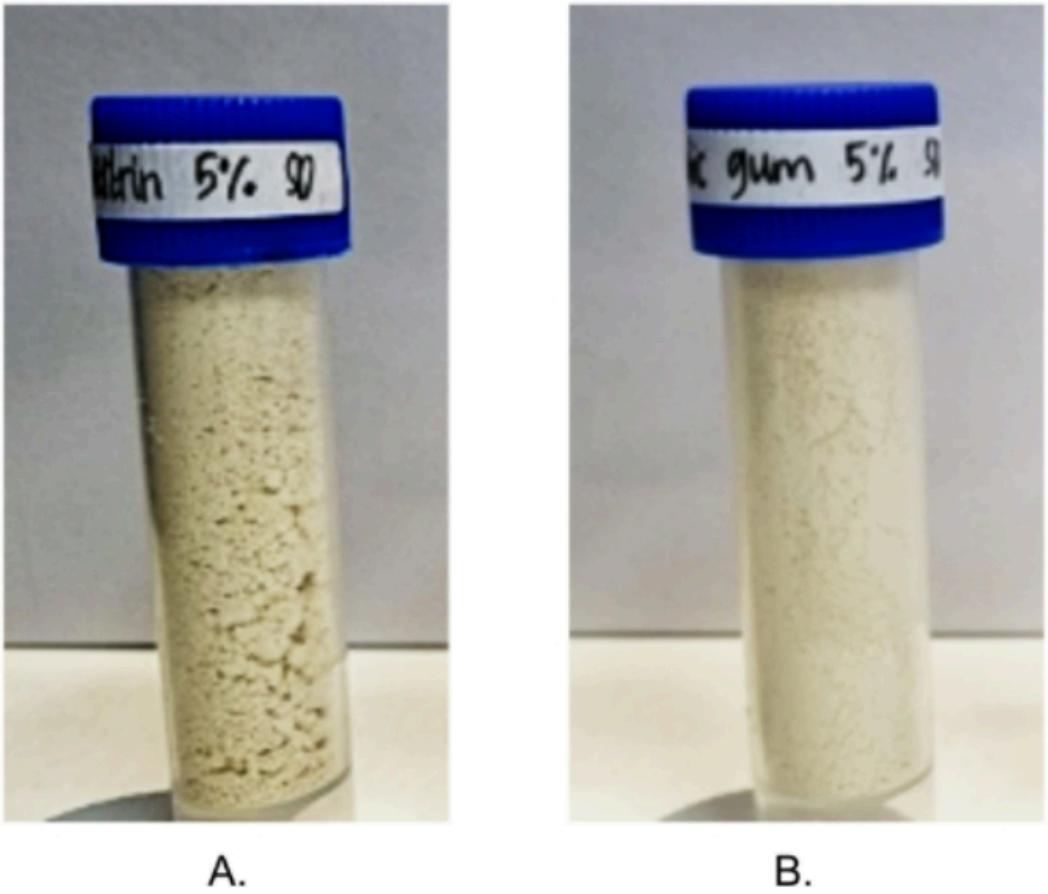


Figure 2

Microencapsulation of crude protease extract from *B. pacificus* HSFI-5 using two different encapsulating agents. A. spray dried product from microencapsulation using 5% b/b maltodextrin; B. spray dried product from microencapsulation using 5% Arabic gum as encapsulating agents.

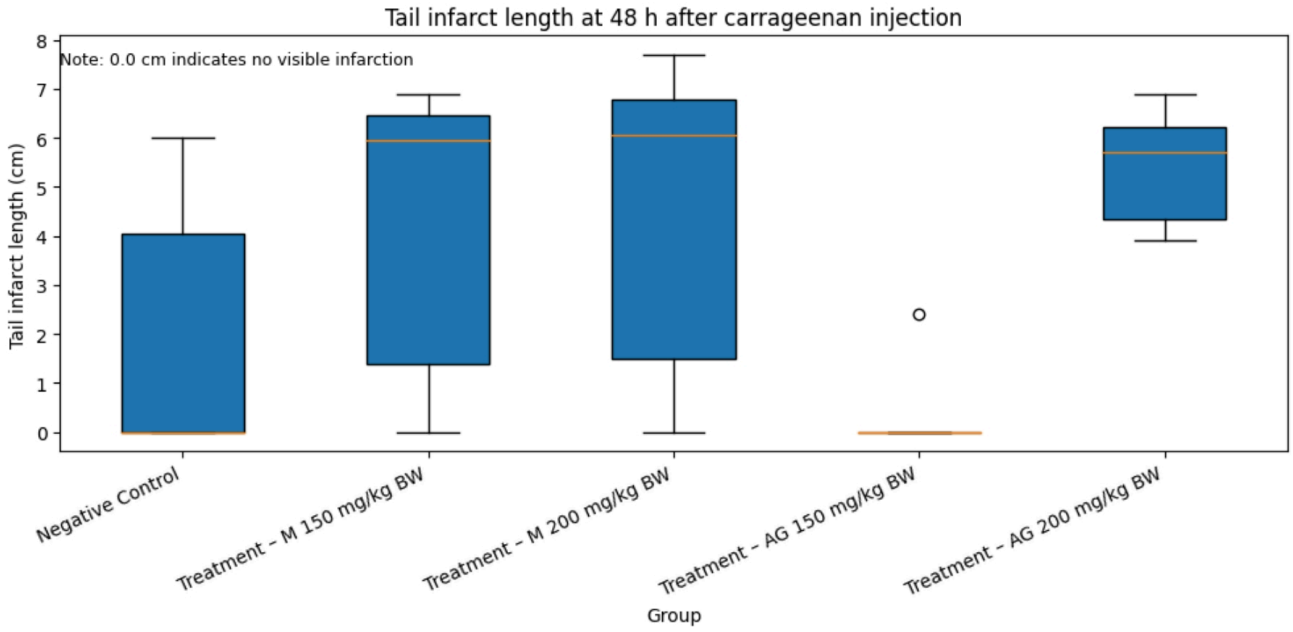


Figure 3

Scatter plot of tail infarct incidences and the length average of mice after 48-h Carrageenan-Induced Thrombosis and oral treatment with Maltodextrin (M) and Arabic gum (AG) microencapsulated fibrinolytic protease at varied dosages. Data are presented as mean ± standard deviation (n = 6 per group), analysis performed using one-way ANOVA (F value = 2.08 and p value = 0.114)

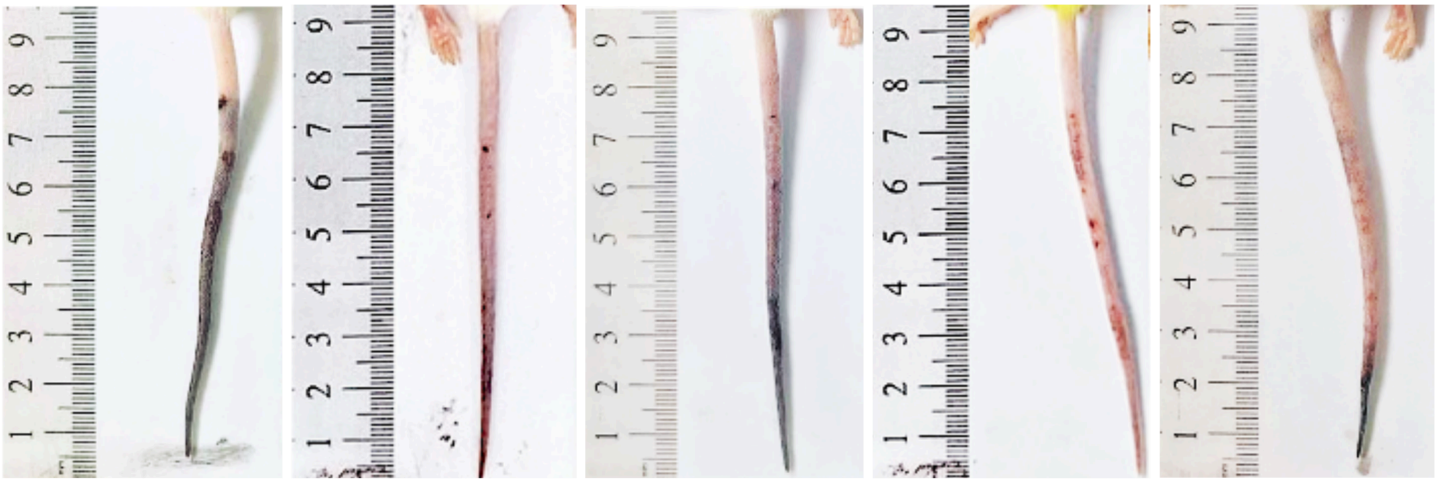


Figure 4

Tail infarct visual representative 48 hours after carrageenan injection and oral treatment with Maltodextrin (M) and Arabic gum (AG) microencapsulated fibrinolytic protease at varied dosages. A, Negative control; B, M 150 mg/Kg BW; C, M 200 mg/Kg BW; D, AG 150 mg/Kg BW; and E, AG 200 mg/Kg BW.

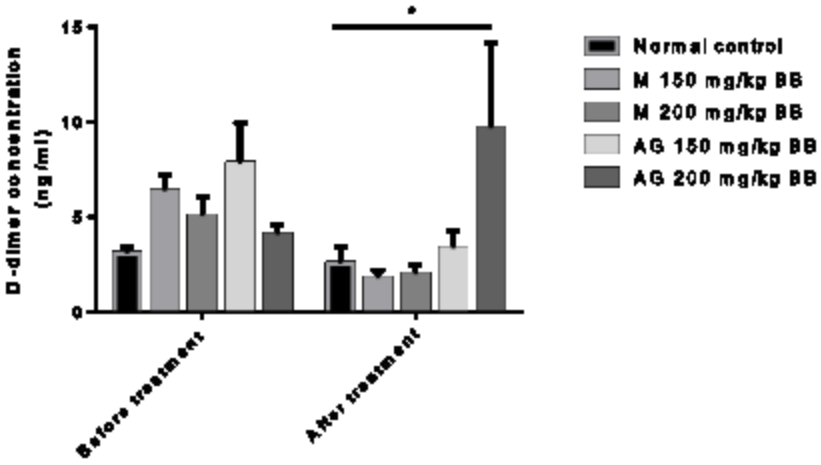


Figure 5

Plasma D-dimer levels following carrageenan-induced thrombosis and administration of fibrinolytic protease from *Bacillus pacificus* HSFI-5. Differences in D-dimer levels among treated groups reflect treatment-associated modulation of fibrin degradation dynamics.

Supplementary Files

This is a list of supplementary files associated with this preprint. Click to download.

- SupplementaryData.pdf
- BacilluspacificusSNE.xls